Presented at Electrochemical Society Meeting,
Boston Massachusetts, November 1–6, 1998,
and submitted to *Proceedings*

Structure and Electrochemical Properties of $LiMn_2O_4$ Thin Films

A. Ueda, J. B. Bates, and R. A. Zuhr
Solid State Division, Oak Ridge National Laboratory
P.O. Box 2008, Oak Ridge, Tennessee 37831-6030

prepared by
SOLID STATE DIVISION
OAK RIDGE NATIONAL LABORATORY
Managed by
LOCKHEED MARTIN ENERGY RESEARCH CORP.
under
Contract No. DE-AC05-96OR22464
with the
U.S. DEPARTMENT OF ENERGY
Oak Ridge, Tennessee

December 1998

DISCLAIMER

Lithium Battery Proceedings volume
of the 1998 ECS fall meeting

STRUCTURE AND ELECTROCHEMICAL PROPERTIES OF $LiMn_2O_4$ THIN FILMS

Atsushi Ueda, J. B. Bates, and R. A. Zuhr

Solid State Division,
Oak Ridge National Laboratory,
P.O. Box 2008
Oak Ridge, Tennessee 37831-6030, U.S.A.

Key words: solid-state lithium batteries, thin-film batteries, $LiMn_2O_4$, defect spinel structure

STRUCTURE AND ELECTROCHEMICAL PROPERTIES OF $LiMn_2O_4$ THIN FILMS

Atsushi Ueda, J. B. Bates, and R. A. Zuhr

Solid State Division, Oak Ridge National Laboratory,
P.O. Box 2008, Oak Ridge, Tennessee 37831-6030, U.S.A.

ABSTRACT

The structural and electrochemical properties of $LiMn_2O_4$ films depend upon the deposition and annealing conditions. Films which were deposited by rf magnetron sputtering of $LiMn_2O_4$ in Ar + N_2 gas mixtures and annealed in O_2 at temperatures between 400 to 1000°C had the cubic spinel structure with an a-axis length that increased linearly from 8.13 to 8.25 Å with increasing anneal temperature. Thin-film lithium cells with cathodes of different a-axis lengths exhibited marked differences in their voltage profiles. In particular, the ratio of the capacities at 4 V and 3 V increased with the a-axis length. A defect model of $LiMn_2O_4$ which is consistent with the structural and electrochemical data is represented by

$$[Li_{1-y+z}Mn^{2+}_{y-z}]_{8a}[Mn^{2+}_{z}]_{16c}[Li_xMn_{2-x}]_{16d}O_4.$$

Based on this model and the results of in-situ XRD measurements, it is proposed that Mn ions migrate from 8(a) tetrahedral sites to 16(c) octahedral sites on charging the cells in the 5V plateau.

INTRODUCTION

Thin films of crystalline $LiMn_2O_4$ have been prepared in our laboratory by e-beam evaporation and rf-magnetron sputtering of $LiMn_2O_4$ targets followed by heat treatment in O_2 at elevated temperatures (1-3). In addition to the characteristic voltage plateaus at 3 V and 4 V, thin film lithium cells typically exhibited significant capacity at 5 V and, depending on the deposition and processing conditions, at 4.6 V. Several models based on inverse spinel structures have been proposed to explain the 5 V and 4.6 V plateaus (3-5). It is the purpose of this research to build on these ideas to develop a defect model of crystalline $LiMn_2O_4$ films that is consistent with all of the electrochemical and structural data. Of particular interest is the apparent migration of Mn ions from the tetrahedral 8a sites to the 16c octahedral on charging in the 5 V plateau and the two-phase reaction that takes place on charging at 4.6 V in which the monoclinic form of $LiMn_2O_4$ is converted irreversibly to the spinel structure.

RESULTS AND DISCUSSION

Structural Properties of $LiMn_2O_4$ Thin Films

Films of $LiMn_2O_4$ about 0.3 to 0.5 μm thick were deposited over Pt current collectors on alumina substrates by rf magnetron sputtering of $LiMn_2O_4$ in Ar + 10% N_2 gas mixtures. The as-deposited x-ray amorphous films were crystallized by annealing at 400°C to 1000°C in flowing O_2 at heating and cooling rates of 5°C/min.

Near grazing angle (3° incidence angle) X-ray diffraction patterns observed after annealing films deposited in $Ar + N_2$ at 400-1000°C are shown in Fig. 1. The lines due to the alumina substrate and Pt current collector are marked in the upper trace. In addition to the major reflections indicated, the weak (2,2,0) line also was observed after annealing at 1000°C. For films less than 0.5 μm thick, the diffraction patterns could be indexed in the cubic setting for a single spinel phase. For thicker films, the diffraction patterns were consistent with the monoclinic structure (7). Possibly this conversion to the monoclinic structure is driven by the tendency to minimize volume strain energy during annealing. For the $LiMn_2O_4$ films deposited in an $Ar + O_2$ mixture, diffraction lines of the cubic spinel phase and the monoclinic phase were observed. As demonstrated by the decrease in the line width, the crystallinity (grain size) of the films increased with annealing temperature, and the diffraction line shifted toward lower angles. The *a*-axis lengths determined from a least squares fit to the major reflections increased linearly with annealing temperature from 8.13 to 8.25 Å, as can be seen in Fig. 2.

The Mn/O ratios determined from RBS measurements of as-deposited and 400°C annealed films were 0.45(±0.02), indicating that the films are manganese deficient.

Electrochemical Properties of $LiMn_2O_4$ Thin Films

After characterizing the $LiMn_2O_4$ thin films, thin film cells were constructed following the procedures summarized elsewhere (1,2). The cathodes were covered with about 1.5 μm thick films of the amorphous lithium phosphorous oxynitride (Lipon) electrolyte. This material has a lithium ion conductivity of $2(\pm1) \times 10^{-6}$ S/cm and is stable from 0 to about 5.5 V. vs. lithium metal at room temperature (8). Lithium metal anode films about 3 μm thick were deposited over the electrolyte by evaporation of lithium metal, and the cells were sealed under argon in stainless steel jars. Electrochemical tests were carried out using a Maccor battery test system with high impedance channels.

Charge-discharge curves of cells with cathodes which were annealed at 400°C and 800°C and had different a-axis lengths (**a**) are shown in Fig. 3. As can be seen in the figure, these cells exhibited significant differences in their capacities at 4 V and 5 V relative to the capacity at 3 V. With increasing a-axis length (increasing annealing temperature), the relative 4 V and 5 V capacities increased and decreased, respectively (Table 1). Typical of cells with single phase cubic spinel cathodes deposited by sputtering in $Ar + N_2$, the plateau at 4.6 V was not observed. On the otherhand, cathodes that were deposited in $Ar + O_2$ process gas mixtures consisted of a mixed phase of monoclinic and cubic $LiMn_2O_4$, and all of the cells with these cathodes exhibited a long 4.6 V plateau (7) on the first charge.

Structure Model of $LiMn_2O_4$ Thin Films

The ratios of capacities at 4 V and 3 V increased with the a-axis length, as shown in Fig. 4. This behavior is similar to that of Li rich (manganese deficient) defect spinel (6):

$$[Li]_{8a}[Li_xMn_{2-x}]_{16d}O_4 \qquad (1)$$

Using bulk data for the 4V/3V capacity ratio vs. a-axis length (6), the defect model qualitatively fits the thin-film data as shown by the solid curve in Fig. 4. At the end of 4 V region (4.5 V state), all of manganese ions are teravalent. Further extraction of lithium from the defect structure in Eq.(1) could result from one of the two following conditions: (i) Mn^{4+} is oxidized to Mn^{5+} or (ii) the cathode decomposes with oxygen release. However, we have found no evidence for either event.

Several models have been proposed to explain the origin of the 5 V-plateau (3-5) including simple mixed inverse spinels. We propose the following defect model represented by

$$[Li_{1-y+z}Mn_{y-z}]_{8a}[Mn_z]_{16c}[Li_xMn_{2-x}]_{16d}O_4 \quad (2)$$

where Li^+ and Mn ions are located on tetrahedral 8a(Mn^{2+}), octaheral 16c(Mn^{2+}) sites, and octahedral 16d sites (Mn^{4+},Mn^{3+}). The 3 V region results from the insertion of 1 Li^+ per 4 O^{2-} ions into the 16c sites accompanied by the reduction of an equal number of Mn^{4+} to Mn^{3+}. In the 4 V region, all of the Mn^{3+} ions are oxidized to Mn^{4+} as 1 - 3 x + y + z Li^+ ions are extracted from the 8a sites. We speculate that the 5 V plateau arises from the extraction of the remaining 2y Li^+ from the 8a sites accompanied by the oxidation of the Mn^{2+} ions on these sites. From the relative capacities, the values of x and y were calculated for z = 0, and the results are given in Table 1.

Table 1. Estimation of the compositions of $LiMn_2O_4$ films based on nonstoichiometric defect spinel model of $[Li_{1-y+z}Mn^{2+}{}_{y-z}]_{8a}[Mn^{2+}{}_z]]_{16c}[Li_xMn_{2-x}]_{16d}O_4$ (z = 0).

Annealing temperature / °C	a-axis / A	Capacity Ratio R_1 4V/3V	R_2 5V/3V	x*	y*
400	8.12	0.21	0.64	0.37	0.32
600	8.16	0.50	0.39	0.23	0.20
800	8.18	0.58	0.25	0.18	0.13

* $1 - 3x + y = R_1$, $2y = R_2$

The value of z gives the distribution of Mn^{2+} ions between 8(a) and 16(c) sites. The relative intensities of the (3,1,1) and (1,1,1) reflections are sensitive to this distribution, and from the observed intensity ratios of (3,1,1)/(1,1,1) we find that the density of Mn^{2+} on 8(a) site increased (value of z decreased) with the increase in annealing temperature.

In-situ XRD Study in the 5 V Plateau

In order to characterize the 5V reaction, in-situ XRD measurements were made. The cell was based on a $LiMn_2O_4$ thin film annealed at 750°C, and a multilayer coating of parylene and titanium films was deposited over the lithium anode to protect it from air. As can be seen in Fig.5, the position of the (1,1,1) diffraction line increased on charging from 3.8 V to 4.5 V but remained fixed on continued charging in the 5 V plateau. This means that the lattice size did not change on extracting lithium ions at 5 V. Changes in the intensities of the (1,1,1), (3,1,1), and (4,0,0) diffraction were observed during the reaction, as shown in Table 2. The facts that the intensities of (1,1,1) and (3,1,1) increased and decreased, respectively, on charging in the 5 V plateau while the cell volume remained fixed and that the capacity at 5 V decreased significantly on the following discharge cycle suggest that the Mn ions on the 8(a) tetrahedral sites migrated to 16(c) octahedral sites.

Table 2. Change in the locations and intensities of (1,1,1), (3,1,1), and (4,0,0) during the 5V-reaction.

		Relative intensity†		
CCV	OCV	(1,1,1)	(3,1,1)	(4,0,0)
4.5 V	4.302 V	133	75	100
5.0 V	4.405 V	100	100	100
5.3 V	4.350 V	138	80	105

†Each relative intensity was determined based on the 5.0 V-state.

CONCLUSIONS

The structural and electrochemical properties of crystalline $LiMn_2O_4$ films depend upon the deposition and annealing conditions. Films deposited by rf magnetron sputtering of $LiMn_2O_4$ in Ar + 10 % N_2 gas mixtures and annealed in O_2 at 400°C to 1000°C exhibited a single phase cubic spinel structure with an a-axis length that increased linearly with annealing temperature from 8.13 Å to 8.25 Å.

Cells with cathodes having different **a** values exhibit marked differences in their relative capacities at 3 V, 4 V, and 5 V. In particular, the ratios of capacities at 4 V and 3 V increased with **a**. This behavior and the origin of the plateau at 5 V can be explained with a nonstoichiometric defect spinel model represented by $[Li_{1-y+z}Mn_{y-z}]_{8a}[Mn_z]_{16c}[Li_xMn_{2-x}]_{16d}O_4$ where the Li ions occupy the tetrahedral 8a and octahedral 16d sites, while the Mn ions occupy the 8a (Mn^{2+}), 16c (Mn^{2+}), and the 16d sites (Mn^{4+}, Mn^{3+}). All of the Mn^{3+} ions are oxidized to Mn^{4+} as 1-3x+y+z Li^+ ions are extracted from the 8(a) sites. We speculate that the 5 V plateau arises from the extraction of the remaining 2y Li^+ from the 8a and 16(d) sites accompanied by the oxidation of the Mn^{2+} ions on these sites and their migration from the 8a sites to the 16c sites.

ACKNOWLEDGMENT

This research was sponsored by the U.S. Department of Energy's Division of Material Sciences and Division of Chemical Sciences under contract No. DE-AC05-96OR22464 with Lockheed Martin Energy Research Corp.

REFERENCES

1. J. B.Bates, D. Lubben, N. J.Dudney, "Thin-Film Li-$LiMn_2O_4$Batteries," *Aerosp. Electron. System. Mag.* **10**, 30 (1995).
2. J. B.Bates, D. Lubben, N. J.Dudney, and F. X.Hart, *J. Electrochem. Soc.* **142**, L149 (1995).
3. J. B. Bates, D. Lubben, N. J. Dudney, R. A. Zuhr, and F. X. Hart, p. 215 in Thin Film Solid Ionics Devices and Materials; 95-22, The Electrochemical Society Proceedings Series (1996).
4. M. M.Thackeray, M. F. Mansuetto, and J. B. Bates, *Solid State Ionics* **68**, 153 (1997).
5. M. M.Thackeray, *J.Electrochem.Soc.***144**, L100 (1997).
6. R. J. Gummow, A. de Kock, and M.M. Thackeray, *Solid State Ionics* **69**, 59 (1994).
7. A. Ueda and J. B. Bates, will be published.
8. X. Yu, J. B. Bates, G. E. Jellison,Jr., and F. X. Hart, *J. Electrochem. Soc.* **144**, 524 (1997).

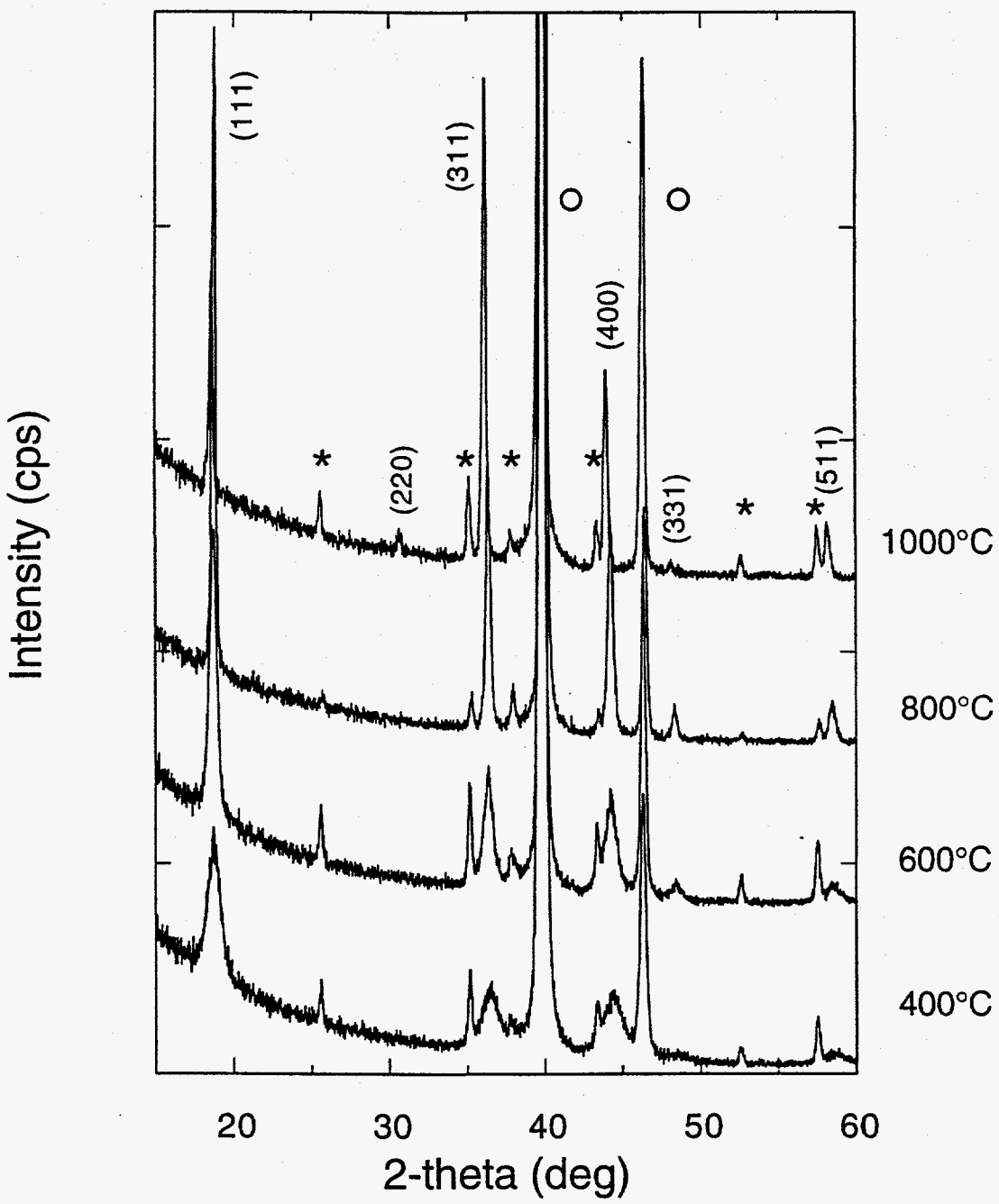

Fig. 1. XRD patterns of $LiMn_2O_4$ thin film annealed at 400 to 1000°C in flowing oxygen. Lines marked by * and ° are due to the substrate and Pt current collector, respectively.

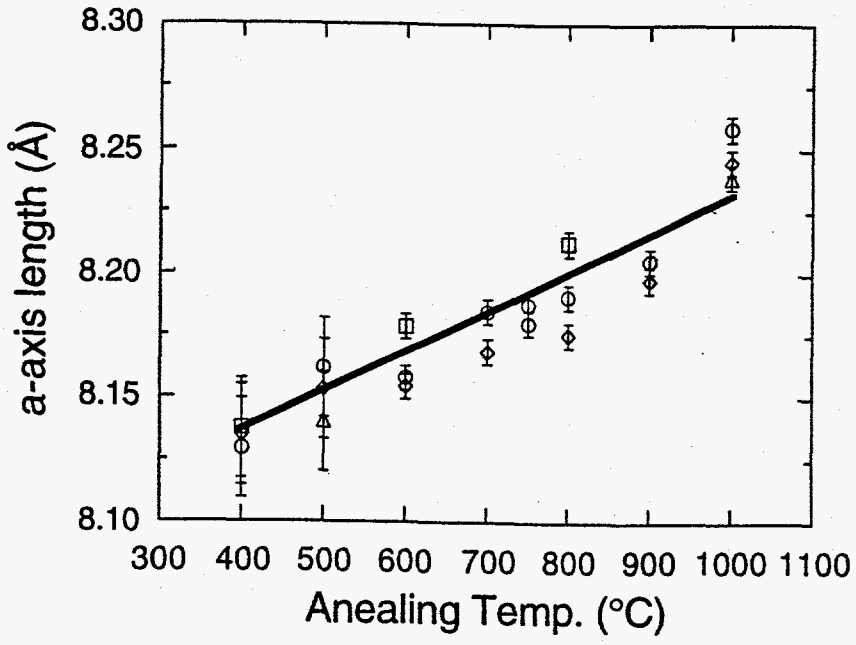

Fig. 2. Change in the a-axis length of $LiMn_2O_4$ thin film with annealing temperature.

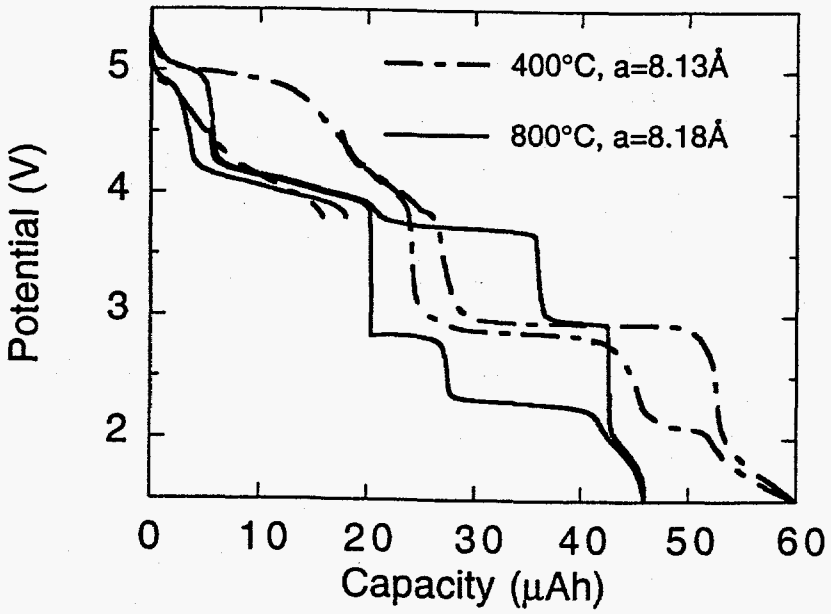

Fig. 3. Low current discharge-charge curves for $Li/LiMn_2O_4$ cells with cathodes annealed at 400 and 800°C.

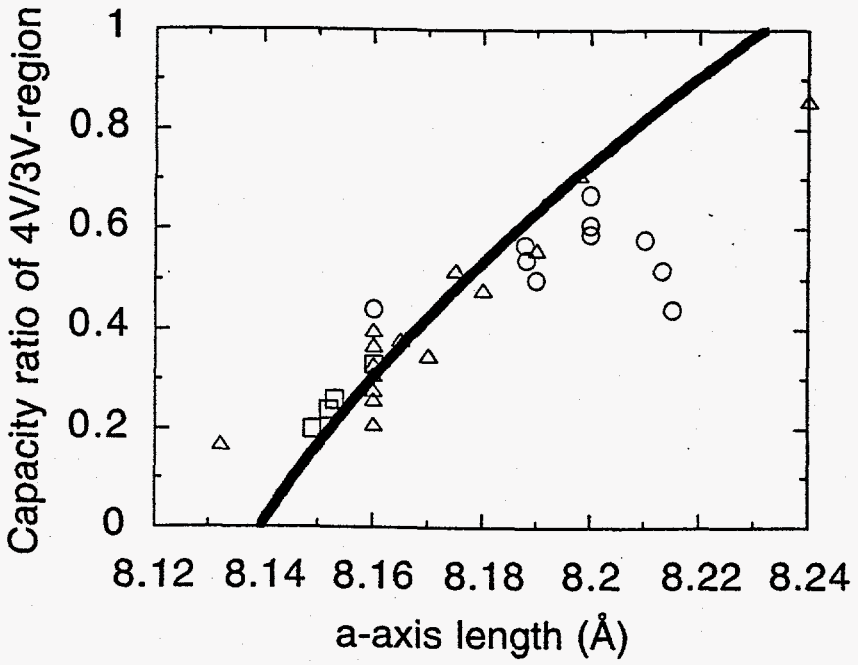

Fig. 4. Measured capacity ratios vs. a-axis length. The solid curve was calculated from a fit of the bulk data for a vs. x in the model $Li[Li_xMn_{2-x}]O_4$.

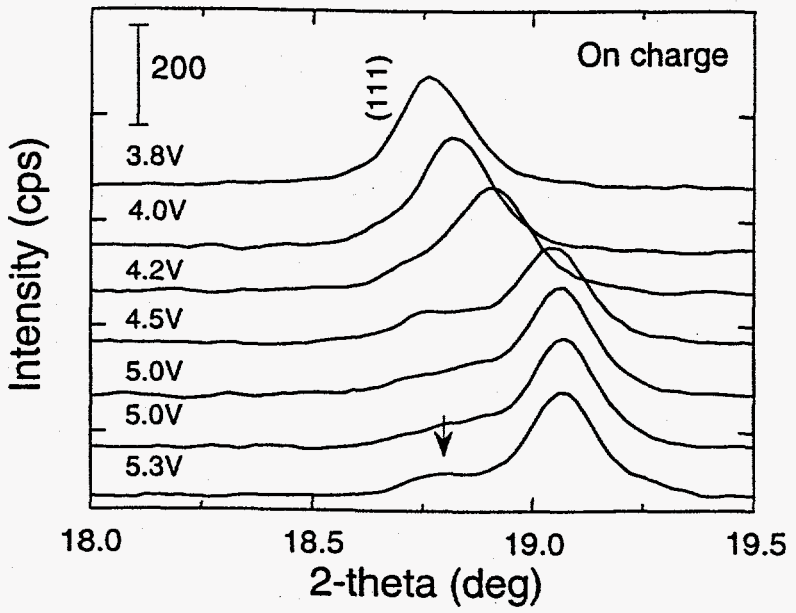

Fig. 5. Change in the (1,1,1) diffraction line in the voltage range of 3.8 to 5.3 V on the charge half cycle. The arrow indicates a weak line that remains fixed after discharge to 1.5 V that is attributed to a small volume fraction of inactive $LiMn_2O_4$.